Mapping carbon stocks in Central and South America using SMAP vegetation optical depth

D. Chaparro[1], G. Duveiller[2], M. Piles[3], M. Vall-llossera[1], A. Cescatti[2], A. Camps[1], D. Entekhabi[4]

[1]Universitat Politècnica de Catalunya, CommSensLab & IEEC/UPC, 08034, Barcelona, Spain.

[2]European Commission, Joint Research Centre, Directorate for Sustainable Resources, Ispra, Italy.

[3]Image Processing Lab (IPL), Universitat de València, 46980, Valencia, Spain.

[4]Department of Civil and Environmental Engineering, Massachusetts Institute of Technology, Cambridge, MA 02139, United States.

This document is a non-peer reviewed preprint. **The final manuscript has been published in the IGARSS 2019 Proceedings: https://ieeexplore.ieee.org/abstract/document/8900244**

To cite this work, please refer to the final version and cite:

Chaparro, D., Duveiller, G., Piles, M., Vall-Llossera, M., Cescatti, A., Camps, A., & Entekhabi, D. (2019, July). Mapping Carbon Stocks In Central And South America With Smap Vegetation Optical Depth. In IGARSS 2019-2019 IEEE International Geoscience and Remote Sensing Symposium (pp. 5449-5452). IEEE. DOI: 10.1109/IGARSS.2019.8900244.

ABSTRACT: Mapping carbon stocks in the tropics is essential for climate change mitigation. Passive microwave remote sensing allows estimating carbon from deep canopy layers through the Vegetation Optical Depth (VOD) parameter. Although their spatial resolution is coarser than that of optical vegetation indices or airborne Lidar data, microwaves present a higher penetration capacity at low frequencies (Lband) and avoid cloud masking. This work compares the relationships of airborne carbon maps in Central and South America with both (i) SMAP L-band VOD at 9 km gridding and (ii) MODIS Enhanced Vegetation Index (EVI). Models to estimate carbon stocks are built from these two satellite derived variables. Results show that L-band VOD has a greater capacity to model carbon variability than EVI. The resulting VOD-derived carbon estimates are further presented at a detailed (9 km) spatial scale.

Keywords: Carbon modelling, vegetation optical depth, tropical forests, L-band, climate change.

1. Introduction

Intact tropical forests are crucial for the mitigation of climate change as they store large amounts of carbon. However, forest degradation counterbalances this effect and leads to a net carbon source in tropical regions [1]. Hence, monitoring the tropical vegetation is essential to assess the carbon budget and model climate change scenarios. Nowadays, satellites are the most efficient tool to monitor carbon changes over large geographic areas. Visible/infrared (VIS/NIR) vegetation indices have been commonly used for this purpose based on their capacity to capture the greenness of vegetation. Complementarily, remote sensing techniques based on laser pulses (i.e., light detection and ranging; LiDAR) captures the forest height and allows a detailed study of carbon stocks. Nevertheless, in both cases there are two main limitations: the masking by clouds and the fact that these measures are mostly sensitive to the top of the vegetation canopy. Passive microwave measurements provide an alternative from which the parameter known as Vegetation Optical Depth (VOD) can be derived. VOD represents the attenuation exerted by the different vegetation layers over microwave emissions. This parameter is tightly linked to the biomass of plants through the vegetation water content (VWC), and provides information from deeper vegetation layers [2]. Forest biomass has been monitored using VOD at C-, X- and K-bands (>4 GHz; [1, 3]). Nevertheless, VOD at L-band (1 to 2 GHz) is expected to improve biomass estimates due to the enhanced penetration capacity of microwaves at lower frequencies. L-band VOD has shown good agreement with vegetation biomass and forest height [4-9]. At present, there are two L-band passive microwave satellite missions in orbit: the ESA's Soil Moisture and Ocean Salinity (SMOS) and the NASA's Soil Moisture Active Passive (SMAP), both with a resolution of ~36 km. This resolution is coarser than that from optical remote sensing techniques and is the main limitation of microwave sensors. SMAP oversampled observations allowed to develop a SMAP enhanced brightness temperature product at 9 km gridding [10] from which VOD at this detailed spatial scale has been derived [5]. In this research, the models to estimate aboveground carbon density (ACD) based on (i) L-band VOD and (ii) the VIS/NIR Enhanced Vegetation Index (EVI) are studied and compared using an enhanced spatial scale (9 km). The study is conducted in Central and South America.

2. Data and methods

2.1. Study area

The study region (Fig. 1) encompasses Panama, southern Colombia, and Peru. This area includes tropical forests in part of the Amazon basin (one of the main carbon reservoirs on Earth) as well as forests, shrublands and grasslands in the Andes (up to ~4,500 m).

2.2. Datasets

2.2.1. Aboveground Carbon Density

The ACD maps (100 m resolution) are produced by the Carnegie Airborne Observatory (CAO) using Lidar sampling between 2010 and 2012, calibration against field plots, and data on precipitation, topography and vegetation [11-13]. The dataset is aggregated to the 9 km gridding of the VOD product (see Section 2.2.2 and Fig. 1a). The uncertainty of these maps is mostly below 10%, especially in the Peruvian forests. More details are provided in [11- 13].

2.2.2. Vegetation Optical Depth

The VOD dataset is retrieved from SMAP Backus-Gilbert brightness temperatures [10] using the Multi-Temporal Dual Channel Algorithm (MT-DCA; [14]) and is provided in the 9 km EASE 2.0 grid. The data used for model calibration and validation span through the first year of SMAP data (April 2015-March 2016) and have been averaged for this period to obtain a single VOD value per pixel (Fig. 1b).

2.2.3. Enhanced Vegetation Index

The EVI data is the 16-day MODIS/Terra MOD13C1 v.6 product, on a 0.05° latitude/longitude global grid, but originally calculated based on reflectances at 250m and 500m spatial resolution . EVI is converted to the EASE 2.0 grid at 9 km scale using bilinear interpolation, and is averaged for the same period as VOD data (April 2015- March 2016, Fig. 1c).

2.3. ACD modelling

The VOD-ACD and EVI-ACD relationships have been calibrated using 70% of pixels in the study area (randomly sampled). As a first approach, power regressions (eqs. (1) and (2)) have been chosen as they provide enhanced fitting than linear regression and allow comparison between the capacities of VOD and EVI to estimate carbon stocks:

$$ACD = a \cdot VOD^{b} \quad (1)$$

$$ACD = a \cdot EVI^{b} \quad (2),$$

where a and b are constant terms. Validation for these models is computed using the remaining 30% of pixels.

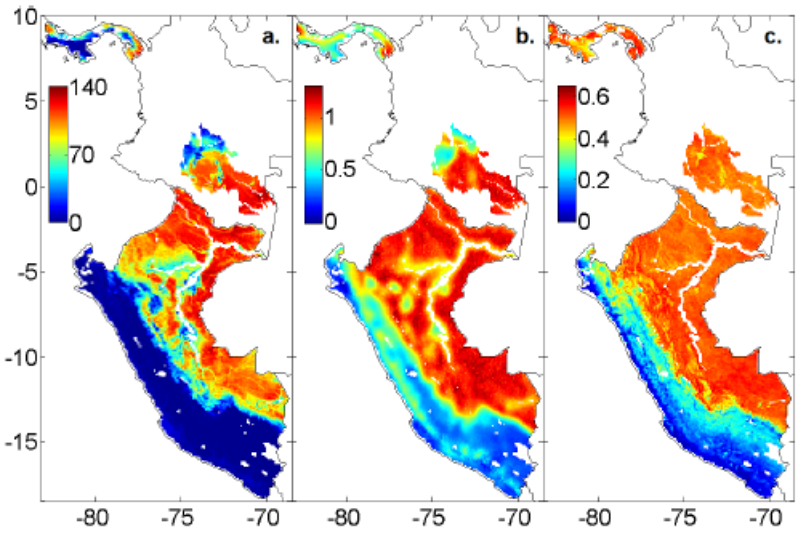

Fig 1. Study area and datasets used. (a) ACD (TC/ha); (b) L-band VOD (dimensionless); (c) EVI (dimensionless).

3. Results

ACD, VOD and EVI maps are shown in Figs. 1a, 1b and 1c, respectively. Both VOD and EVI present their highest values in tropical forest regions (covering most of Peru and the studied area of Colombia), where the highest carbon densities are found. In contrast, lower ACD values are found in the Andes (western Peru), near rivers, and in regions such as Panama and the north of the Colombian region. These patterns match with low VOD values. Instead, EVI decreases only in the Andes. Also, note that EVI saturates in most of the Peruvian tropical forests while VOD shows a larger dynamic range in the region (Fig. 1).

Model fittings are plotted in Fig. 2. The VOD-ACD model (eq. (1)) explains a higher proportion of ACD variance (78%) if compared to the EVI-ACD model (eq. (2); 71%). Importantly, the EVI shows saturation at approximately >40 TC/ha, while there is no saturation evident for L-band VOD.

Validation for both models is shown in Fig. 3. It is found that carbon estimates based on VOD present lower RMSE (22.28 TC/ha) and lower bias (15.52 TC/ha) than those based on EVI (RMSE = 25.68 TC/ha; Bias = 19.64 TC/ha). Finally, Fig. 4 shows the resulting ACD estimates for the study region as an example case.

4. Discussion and future work

The capacity of remote sensing techniques to capture the variability of carbon stocks largely depends on their sensitivity to the biomass of the entire canopy. In that sense, the results reported are consistent with the higher penetration capacity of microwaves in comparison to VIS/NIR indices: the agreement between ACD and VOD is higher (both qualitatively and statistically) than that found for ACD and EVI. The results are also consistent with the lack of saturation for L-band VOD reported in [6, 9]. In that sense, the VOD model explains 78% of the carbon density, while the ACD variance explained by EVI is lower (71%). Similarly, error and bias for the VOD-based model are lower. Therefore, the results reported here show that the applicability of the 9 km VOD dataset to estimate carbon stocks is feasible considering that the

strength and validation of the VOD-ACD relationship is similar to that obtained for coarser resolutions (cf. [8, 15]). Furthermore, the spatial distribution of carbon estimates is consistent with that from airborne Lidar ACD retrievals (Fig. 4). Hence, the use of oversampling measurements and latest advances in optimal interpolation techniques for image reconstruction are particularly promising for microwave radiometry [10, 16]. Future work will be devoted to enhance the model calibration using the four years of SMAP VOD available data, to explore other regression approaches, and to produce ACD maps at 9 km spatial scale to compute carbon balance in tropical regions with high spatial detail.

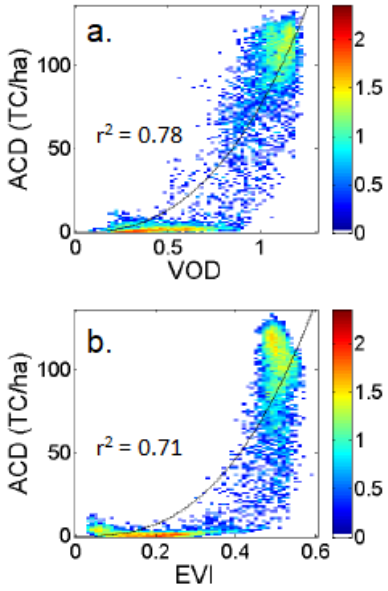

Figure 2. Regressions: (a) ACD as a function of VOD (eq. (1)), and (b) ACD as a function of EVI (eq. (2)). Colorbars show the logarithm of the number of pixels for each ACD-VOD and ACDEVI bin. Binning of variables is used only for display purposes. Binning widths: ACD: 1 TC/ha; VOD: 0.02; EVI: 0.01.

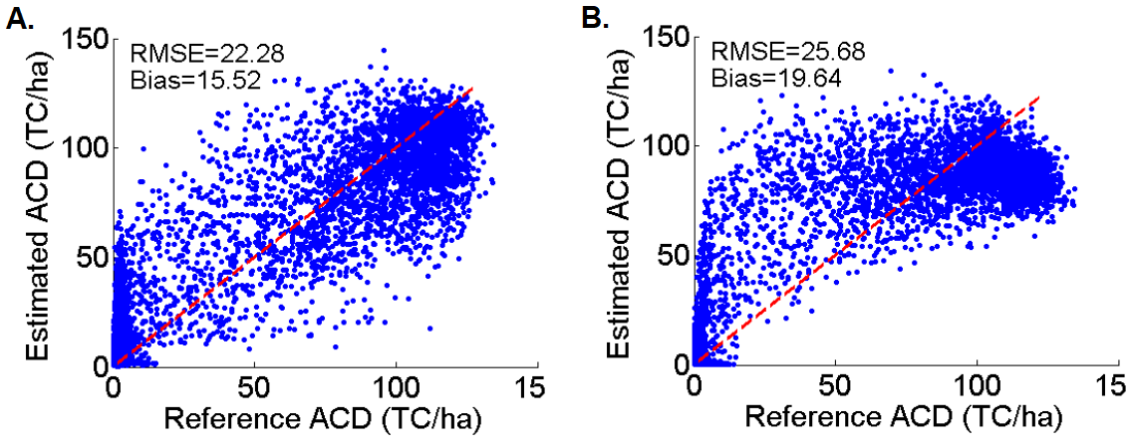

Figure 3. Relationship between reference ACD and estimated ACD for (a) VOD and (b) EVI models.

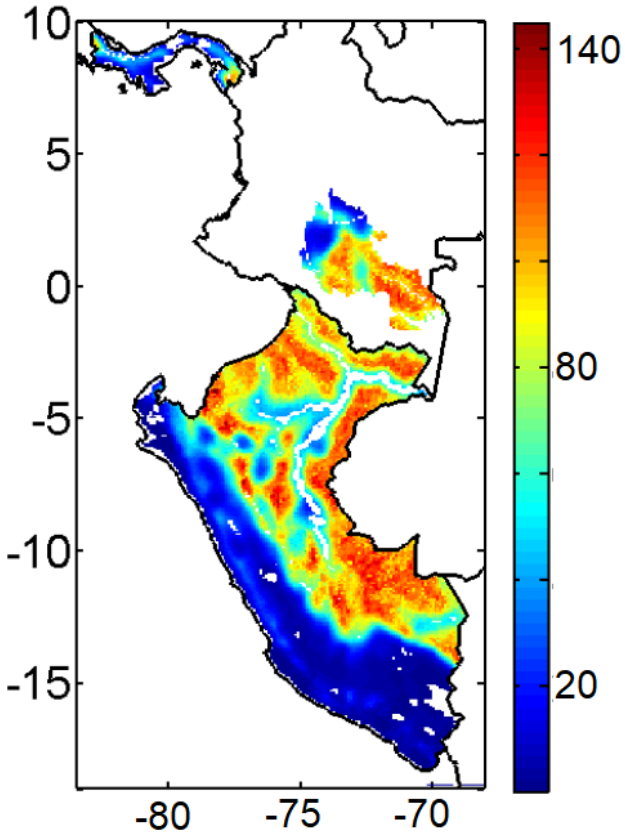

Figure 4. ACD estimates derived from VOD data in the study area. The colorbar shows ACD estimates (TC/ha).

5. Acknowledgements

The L-band VOD data are available from the authors upon request. This study has been supported by the Spanish government through the projects ESP2015-67549-C3-1-R and ESP2017-89463-C3-2-R, and through the award "Unidad de Excelencia María de Maeztu" MDM-2016- 0600, financed by the "Agencia Estatal de Investigación" (Spain). The study has been supported also by the European Regional development Fund (ERDF). Maria Piles is supported by a Ramón y Cajal contract (MINECO) and by the project RTI2018-096765-A-100 (MCIU/AEI/FEDER, UE). We thank the Carnegie Airborne Observatory for making the AGB maps available.

6. References

[1] Y.Y. Liu, A.I. Van Dijk, R.A. De Jeu, J.G. Canadell, M.F. McCabe, J.P. Evans, and G. Wang, "Recent reversal in loss of global terrestrial biomass," *Nature Climate Change*, 5(5), p. 470, 2015. doi: 10.1038/nclimate2581.

[2] Ulaby, F. T., R.K. Moore, and A.K. Fung, *Microwave remote sensing active and passive-Volume III: from theory to applications,* Artech House, Norwood, MA (USA), 1986.

[3] Y.Y. Liu, R.A. De Jeu, M.F. McCabe, J.P. Evans, and A.I. Van Dijk, "Global long-term passive microwave satellite-based retrievals of vegetation optical depth," *Geophysical Research Letters*, 38(18), 2011. doi: 10.1029/2011GL048684.

[4] C. Vittucci, P. Ferrazzoli, Y. Kerr, P. Richaume, L. Guerriero, R. Rahmoune, and G.V. Laurin, "SMOS retrieval over forests: exploitation of optical depth and tests of soil moisture estimates," *Remote Sensing of Environment*, 180, pp. 115-127, 2016. doi: 10.1016/j.rse.2016.03.004.

[5] A.G. Konings, M. Piles, N. Das, and D. Entekhabi, "L-band vegetation optical depth and effective scattering albedo estimation from SMAP," *Remote Sensing of Environment*, 198, 460-470, 2017. doi: 10.1016/j.rse.2017.06.037.

[6] M. Brandt, J.P. Wigneron, J. Chave, T. Tagesson, J. Peñuelas, P. Ciais,..., and N. Rodriguez-Fernandez, "Satellite passive microwaves reveal recent climate-induced carbon losses in African drylands," *Nature Ecology & Evolution*, 2, pp. 827-835, 2018. doi: 10.1038/s41559-018-0530-6.

[7] Chaparro, D., M. Piles, M. Vall-llossera, A. Camps, A.G. Konings, and D. Entekhabi. "L-band vegetation optical depth seasonal metrics for crop yield assessment," *Remote Sensing of Environment*, 212, 249-259, 2018. doi: 10.1016/j.rse.2018.04.049

[8] D. Chaparro, G. Duveiller, M. Piles, A. Cescatti, M. Vallllossera, A. Camps, D. Entekhabi, "Sensitivity of L-band passive microwaves to carbon stocks in tropical forests: a comparison to higher microwave frequencies and optical data." Manuscript under minor revision (Remote Sensing of Environment).

[9] N. Rodríguez-Fernández, A. Mialon, S. Mermoz,... & Kerr, Y. H. (2018). An evaluation of SMOS L-band vegetation optical depth (L-VOD) data sets: high sensitivity of L-VOD to aboveground biomass in Africa. Biogeosciences, 15(14), 4627-4645.

[10] Chaubell, J., *ATBD. SMAP L1B enhancement radiometer brightness temperature data product*, Jet Propulsion Laboratory, California Institute of Technology, 2016.

[11] G.P. Asner, J.K. Clark, J. Mascaro, G.G. García, K.D. Chadwick, D.N. Encinales, ..., and A. Balaji, "High-resolution mapping of forest carbon stocks in the Colombian Amazon," *Biogeosciences*, 9(7), p. 2683, 2012. doi:10.5194/bg-9-2683-2012.

[12] G.P. Asner, J. Mascaro, C. Anderson, D.E. Knapp, R.E. Martin, T. Kennedy-Bowdoin, ..., and C. Potvin, "High-fidelity national carbon mapping for resource management and REDD+," *Carbon Balance and Management*, 8(1), p. 7, 2013. doi: 10.1186/1750-0680-8-7.

[13] G.P. Asner, D.E. Knapp, R.E. Martin, R. Tupayachi, C.B. Anderson, J. Mascaro, ..., and W. Llactayo, "Targeted carbon conservation at national scales with high-resolution monitoring," *Proceedings of the National Academy of Sciences*, 111(47), E5016-E5022, 2014. doi: 10.1073/pnas.1419550111.

[14] A.G. Konings, M. Piles, K. Rötzer, K.A. McColl, S.K. Chan, and D. Entekhabi, "Vegetation optical depth and scattering albedo retrieval using time series of dual-polarized L-band radiometer observations," *Remote Sensing of Environment*, 172, pp. 178-189, 2016. doi: 10.1016/j.rse.2015.11.009.

[15] Vittucci, C., Laurin, G. V., Tramontana, G., Ferrazzoli, P., Guerriero, L., and Papale, D. "Vegetation optical depth at L-band and above ground biomass in the tropical range: evaluating their relationships at continental and regional scales." *International Journal of Applied Earth Observation and Geoinformation*, 77, pp. 151-161, 2019. doi: 10.1016/j.jag.2019.01.006.

[16] V. González-Gambau, E. Olmedo, A. Turiel, J. Martínez, J. Ballabrera-Poy, M. Portabella, and M. Piles, "Enhancing SMOS brightness temperatures over the ocean using the nodal sampling image reconstruction technique," *Remote Sensing of Environment*, 180, pp. 205-220, 2016. doi: 10.1016/j.rse.2015.12.032.